Available online at www.sciencedirect.com
SCIENCE DIRECT
Geochimica et Cosmochimica Acta 70 (2006) 2298–2310
Geochimica
www.elsevier.com/locate/gca

Antimonous acid protonation/deprotonation equilibria in hydrothermal solutions to 300 °C

V.P. Zakaznova-Herzog [a,1], T.M. Seward [a,*]

[a] Institute for Mineralogy and Petrology, ETH Zürich, Swiss Federal Institute of Technology, 8092 Zürich, Switzerland

Received 22 March 2005; accepted in revised form 27 January 2006

Abstract

The ultraviolet spectra of dilute aqueous solutions of antimony (III) have been measured from 25 to 300 °C at the saturated vapour pressure. From these measurements, equilibrium constants were obtained for the following reactions:

$$H_3SbO_3^0 \rightleftarrows H^+ + H_2SbO_3^-$$

for which pK_1 (antimonous acid) decreases from 11.82 to 9.88 over a temperature range from 25 to 300 °C and

$$H_3SbO_3^0 + H^+ \rightleftarrows H_4SbO_3^+$$

for which $\log K_a$ initially decreases from 1.38 at 22 °C with increasing temperature up to 100 °C but then increases until it reaches a value of $\log K_a = 1.8$ at 300 °C. Unionised antimonous acid, $H_3SbO_3^0$, will be the dominant species responsible for antimony transport in low sulphur geothermal fluids in the Earth's crust. In hydrothermal fluids having a high magmatic input, the low pH environment will also encourage the stability of the protonated $H_4SbO_3^+$ species.

1. Introduction

The simple antimonous acid species together with the thioantimonite adducts are considered to be mainly responsible for antimony transport in low oxidation potential geothermal fluids migrating throughout the Earth's crust. Antimony concentrations in hydrothermal fluids are in the range from 0.1 to 0.45 mg/kg (i.e., 0.82–3.70 μmol/dm^3) (Weissberg et al., 1979), whereas ambient temperature natural waters typically contain less than 1 μmol/dm^3 (Filella et al., 2002). Antimony-containing minerals are often abundant in hydrothermal ore deposits but their precipitation chemistry is poorly understood, to a large extent because of the paucity of fundamental data pertaining to the stability and stoichiometry of the relevant species in aqueous media at elevated temperatures and pressures. The aim of this study was thus to obtain thermodynamic information on Sb(III) speciation from ambient to high temperatures in order to be able to predict and model the behaviour of antimony in hydrothermal systems.

In order to be able to study more complex high temperature systems containing antimony (±sulphur), it is necessary to first consider the simple Sb(III) hydrolysis equilibria in aqueous media. However, the aqueous chemistry of antimonous acid, $H_3SbO_3^0$ (or aqueous antimony hydroxide, $Sb(OH)_3^0$), is not well characterised. There are a few published data at 25 °C but almost no data are available at high temperatures.

Two equilibria may be defined, which describe antimonous acid protonation/deprotonation in aqueous solutions; i.e.,

$$H_3SbO_3^0 + H^+ \rightleftarrows H_4SbO_3^+ \quad K_a \qquad (1)$$

* Corresponding author. Fax: +41 1632 1088.
E-mail addresses: herzog@erdw.ethz.ch (V.P. Zakaznova-Herzog), tseward@erdw.ethz.ch (T.M. Seward).
[1] Present address: Institute of Isotope Geochemistry and Mineral Resources, ETH Zürich, Swiss Federal Institute of Technology, Zürich, Switzerland.

0016-7037/$ - see front matter © 2006 Elsevier Inc. All rights reserved.
doi:10.1016/j.gca.2006.01.029

$$H_3SbO_3^0 \rightleftarrows H^+ + H_2SbO_3^- \quad K_1 \qquad (2)$$

where K_a and K_1 are the equilibrium constants for reactions (1) and (2), respectively. The published experimentally derived thermodynamic data for antimonous acid ionisation (K_a and K_1) at 25 °C are summarised in Table 1. Throughout this paper, we write the Sb(III) hydrolytic equilibria as acid ionisation as defined by Eqs. (1) and (2) bearing in mind the strong acidic properties of antimony (III) at low pH.

Antimony (III) oxide solubility at ambient temperature has been studied by Gayer and Garrett (1952) in water, sodium hydroxide, and hydrochloric acid solutions under nitrogen atmosphere. The solubility of antimonous trioxide in water was found to be 5.2×10^{-5} mol/kg. In basic solutions, the solubility increases to 99.8×10^{-5} mol/kg. Solubility also increases in acidic media to 10.2×10^{-5} mol/kg. We have derived values for pK_a and pK_1 from data of Gayer and Garrett (1952) and these values are given in Table 1. Baes and Mesmer (1976) refer to the value of Mishra and Gupta (1968) as the most precisely known stability constant for antimonous acid protonation at that time.

Jander and Hartmann (1965) and Ahrland and Bovin (1974) determined the speciation of antimony (III) in aqueous solutions at ambient temperature. Jander and Hartmann (1965) carried out ionophoresis, ion exchange, and diffusion measurements at very high ionic strength in basic (16 M NaOH) and acidic (11 M $HClO_4$) media and demonstrated that there were apparently no polymeric species formed and that one species ($H_2SbO_3^-$) existed in basic solutions and one in acidic solutions ($H_4SbO_3^+$). Ahrland and Bovin (1974) studied the hydrolysis of antimony (III) in perchloric and nitric acid solutions at ionic strength $I = 5$ M at 25 °C using the solubility method. The recalculated values for the ionisation and protonation reactions from the potentiometric and solubility studies of Vasil'ev and Shorokhova (1972, 1973) are given in Table 1. At elevated temperatures, the only reported values for the ionisation and protonation constants of antimonous acid are from the solubility study (to 200 °C) of Popova et al. (1975). Zotov et al. (2003) measured the solubility of antimony trioxide up to 450 °C and pressure up to 1000 bar but considered the presence of only one species, $Sb(OH)_3$. Our study therefore focuses on the determination of the equilibrium constants for antimonous acid protonation/deprotonation at temperatures from 22 to 300 °C at equilibrium saturated vapour pressure.

2. Experimental methods

Antimony trioxide behaves as a hydrophobic solid and is sparingly soluble in water (5.2×10^{-5} m at 25 °C and 1 bar; Gayer and Garrett, 1952). In addition, Sb(III) solutions are sensitive to the presence of atmospheric oxygen, forming Sb(V). Thus, some considerable care must be taken in the preparation of Sb(III)-containing solutions. Sb_2O_3 was dissolved in degassed water (double distilled in silica glass) under an argon atmosphere at 65 °C, allowing up to 3 days to yield either saturated or near saturated solutions. Solutions were then filtered under an argon atmosphere. The degassing (no CO_2 or O_2) was carried out in an ultrasonic bath by repeated evacuation from a sealed flask and subsequent purging with argon. Oxidation of Sb(III) can occur because of trace oxygen impurities in the argon gas due to the long time (days) required for dissolving antimony trioxide. Gmelin (1950) suggested boiling Sb_2O_3 in water under argon for 24 h but in our experience, this method proved vulnerable to the intrusion of O_2 into the solution, causing the formation of Sb(V). For solubility measurements, this may be a minor effect but for spectrophotometric measurements it is critical, because Sb(V) species also absorb intensely in the ultraviolet region. All solutions in this study were prepared with high purity Ar (Ar 6.0 grade) which had been further purified by passing the argon through a column of elemental copper filings maintained at 400 °C. The antimony concentrations of both saturated and unsaturated stock solutions were determined by atomic absorption analysis with a precision ±2%. The solutions used for spectrophotometric measurements were prepared by dilution by weight with deoxygenated water under an argon atmosphere.

The compositions of all the solutions used in this study are given in Appendix A. $HClO_4$ and NaOH stock solutions used for spectrophotometric titrations were standardized under deoxygenated argon by acid/base titration using tris-hydroxymethyl-aminomethane with phenolphtalein for the acid and potassium hydrogen phthalate (KHP) with methyl orange for the base.

Spectrophotometric titrations were used to obtain Sb solution spectra from 22 to 75 °C, using an experimental set-up as shown in Fig. 1. A titration vessel (with Sb-containing solutions under constant Ar flow) was connected with the automatic titrator (Metrohm), HPLC pump (Dynamax, Varian), and a flow-through quartz glass cuvette. This cuvette was placed within a Cary 5

Table 1
Previously reported values for protonation/ionisation constants of antimonous acid at ambient temperature

t (°C)	pK_a	pK_1	I	Method	References
25	−1.17	11.78	0	Solubility	Gayer and Garrett (1952); recalc.
25	−1.19	—	5 M	Solubility	Ahrland and Bovin (1974); recalc.
25	−1.42	—	0	Spectroph.	Mishra and Gupta (1968)
25	−1.30	—	0	Potent.	Vasil'ev and Shorokhova (1972); recalc.
25	—	11.75	2 M	Solubility	Vasil'ev and Shorokhova (1973); recalc.
25	−1.49	11.92	0	Solubility	Popova et al. (1975)

M = mol/dm^3.

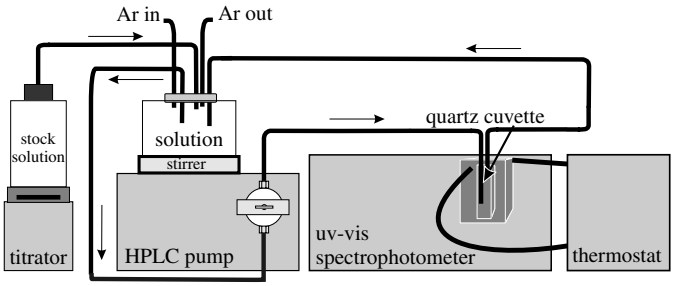

Fig. 1. Experimental set-up used from 22 to 75 °C.

Spectrophotometer (Varian) and the temperature regulated from 22 to 75 °C(±0.1 °C). The automatic titrator added fixed amounts of stock ($HClO_4$ or NaOH) solution in a titration vessel to change pH of the solution. After each titration step, the stirred solution was pumped from the titration vessel into an optical cuvette and a spectrum was collected. From the optical cuvette, the solution was then pumped back to the titration vessel, keeping the total solution volume in the experiment constant. A "dead volume" comprising the solution within the cuvette and tubes was measured and taken into account in the titrations. All connecting tubing was made from Teflon.

The experimental facility used for the high temperature spectrophotometric measurements (from 150 to 300 °C) is similar to the one described previously (Zakaznova-Herzog et al., in press). The solutions were prepared as described above, however, after each measurement, the solutions were not returned to the original solution reservoir because of the possibility of a contamination from the stainless steel outlet tubing (the inlet is lined with gold). The spectra were collected in a flow-through mode at all temperatures.

Thus, spectra were obtained from 22 to 300 °C over a wide range of pH from 0.8 to 12.5 and Sb(III) concentrations around 0.0001 mol/dm^3 (see Appendix A), and corrected for background absorbance (i.e., water and quartz windows). To relate the molar concentration scale of the Beer–Lambert law to the molal scale of standard thermodynamic convention, the measured absorbances, A^{obs}, were corrected for the isothermal variation of solution density at each temperature. The solutions were all in the dilute range and were treated as water with the required density data being taken from Haar et al. (1984).

3. Results and discussions

3.1. Spectra interpretation

Interpretation of the spectra obtained from antimony-containing solutions with pH from 9 to 12.5 is similar to the procedure outlined in our previous study of arsenous acid (Zakaznova-Herzog et al., in press). Fig. 2 shows the calculation scheme used in this study. Absorbance is a linear function of the concentrations of all absorbing species at a given wavelength. The number of independent columns in the absorbance matrix (i.e., the rank) gives the number of absorbing species. Thus, the first step after creating the absorbance matrix (A^{obs} with "i" number of solutions and "k" number of measured wavelength points), is to determine the rank of the matrix. Establishing the number of absorbing species allows one to create a chemical model, which in turn is used to develop a mathematical model based on the charge and mass balance relations and the various equilibrium constant expressions.

The mathematical model for antimonous acid speciation requires consideration of mass and charge balance expressions at:

(a) low pH

mass balance:

$$[Sb] = [H_4SbO_3^+] + [H_3SbO_3^0] \quad (3)$$

charge balance:

$$[H_4SbO_3^+] + [H^+] + [Na^+] = [OH^-] + [ClO_4^-] \quad (4)$$

and also mass action:

$$K_a = \frac{[H_4SbO_3^+]\gamma_{H_4SbO_3^+}}{[H^+]\gamma_{H^+}[H_3SbO_3^0]}\gamma_{H_3SbO_3^0} \quad (5)$$

$$K_w = [H^+]\gamma_{H^+}[OH^+]\gamma_{OH^-} \quad (6)$$

(b) high pH

mass balance:

$$[Sb] = [H_3SbO_3^0] + [H_2SbO_3^-] \quad (7)$$

charge balance:

$$[H^+] + [Na^+] = [OH^-] + [H_2SbO_3^-] \quad (8)$$

mass action:

$$K_1 = \frac{[H_2SbO_3^-]\gamma_{H_2SbO_3^-}[H^+]\gamma_{H^+}}{[H_3SbO_3^0]\gamma_{H_3SbO_3^0}} \quad (9)$$

and additionally, NaOH association defined by

$$K_{ass} = \frac{[NaOH]\gamma_{NaOH}}{[Na^+]\gamma_{Na^+}[OH^-]\gamma_{OH^-}} \quad (10)$$

and again, the ion product constant of water, i.e., Eq. (6). The terms in square brackets are molar concentrations of species in mol/dm^3; γ is the activity coefficient. The necessary activity coefficients were calculated using an extended Debye–Hückel equation (e.g., Robinson and Stokes, 1968)

$$\log \gamma_i = \frac{-Az_i{}^2\sqrt{I}}{1 + \mathring{a}B\sqrt{I}}, \quad (11)$$

where A constant was taken from Bradley and Pitzer (1979) (corrected to molar scale) and B constant was taken from Helgeson and Kirkham (1974); å was estimated by analogy from Kielland (1937). It should be noted that the ionic strength of most of solutions studied was always $\leqslant$0.01.

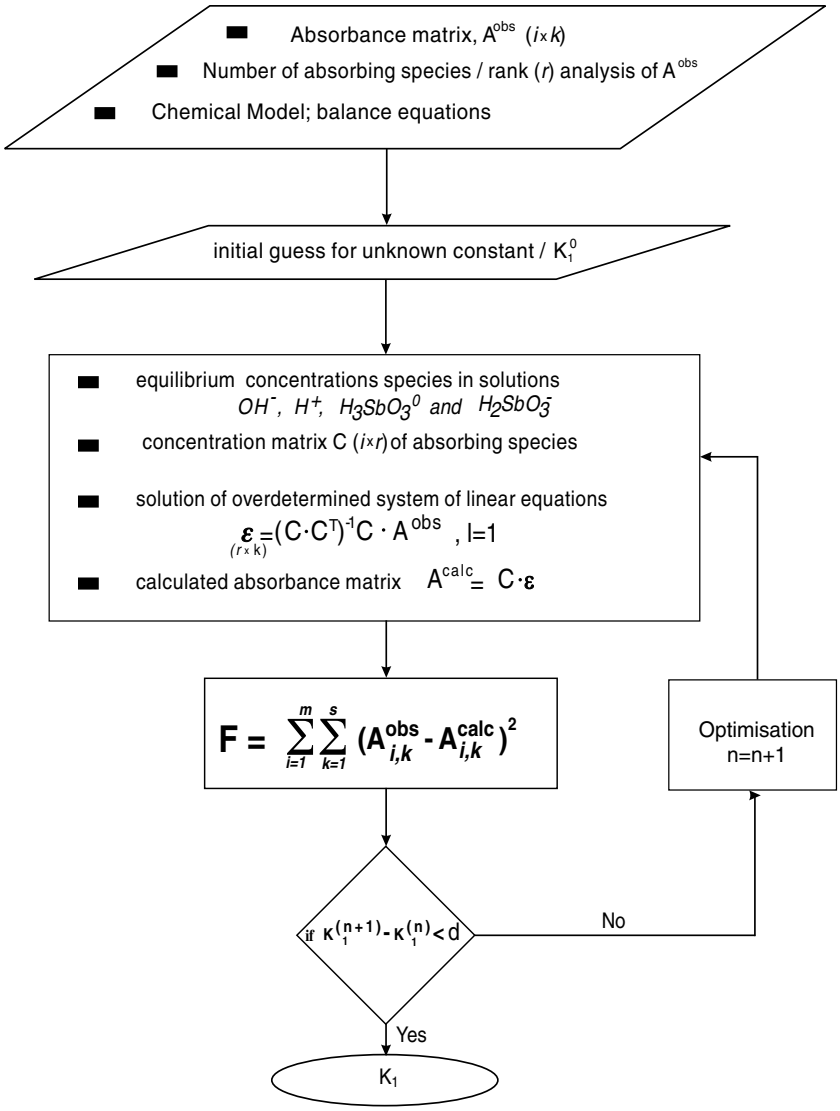

Fig. 2. Computational scheme for calculation of the ionisation constant.

The association constant for sodium hydroxide ion pairing was taken from Ho et al. (2000).

Assuming a value for K_a and taking the values for the other equilibrium constants as known, the mass and charge balance equations can be solved and concentrations of all existing species in the solution calculated. The next step involves the calculation of molar absorptivities, using the constrained non-negative least squares method of optimisation. The optimisation is constrained such that the molar absorptivities are positive, (i.e., there is no negative absorbance). Thus, the theoretical absorbance can be calculated. After this, a second optimisation process determines the least squares minimum, with care being taken to avoid values of the equilibrium constant corresponding to a local minimum. This can occur when the initial guesses are wrong or too divergent from the real value.

Uncertainty calculations were done using the Gaussian error propagation rule

$$\sigma_K = \sqrt{\left(\frac{\partial K}{\partial [\mathrm{Sb}]}\sigma_{[\mathrm{Sb}]}\right)^2 + \left(\frac{\partial K}{\partial [\mathrm{Na}]}\sigma_{[\mathrm{Na}]}\right)^2 + \left(\frac{\partial K}{\partial K_w}\sigma_{K_w}\right)^2}, \quad (12)$$

where $\partial K/\partial[\mathrm{Sb}], \partial K/\partial[\mathrm{Na}], \partial K/\partial K_w$ are the partial derivatives of an ionisation constant with respect to each given parameter [i.e., total antimony concentration, total sodium concentration (or total perchlorate concentration)] and the ionisation constant of water, respectively. $\sigma_{[\mathrm{Sb}]}$, $\sigma_{[\mathrm{Na}]}$, σ_{K_w} are standard deviations of total antimony concentration, total sodium concentration (or total perchlorate concentration), and the ionisation constant of water.

Partial derivatives were obtained using a "brute-force" approach with a "central differences" method. For example, the partial derivative of K with respect to the parameter [Sb] at a point $[\mathrm{Sb}]_i$ is estimated by solving the model (optimisation) at two points ($[\mathrm{Sb}]_i - h$) and ($[\mathrm{Sb}]_i + h$), where h is a

small number (e.g., 1×10^{-9}) and the respective outputs are obtained as K_{i1} and K_{i2}. The partial derivative is then given by

$$\frac{\partial K}{\partial[\mathrm{Sb}]} \approx \frac{K_{i1} - K_{i2}}{2h}, \quad h \to 0. \tag{13}$$

In the same way, the partial derivative of K with respect to other parameters such as [Na] and the ionisation constant of water are obtained. Each spectrum was obtained at a different antimony and sodium concentration with different corresponding uncertainties. This means that the partial derivative of K with respect to each parameter's value with a given standard deviation has to be taken into account. This was done by taking an average value of all partial derivatives with respect to one parameter, multiplied by its standard deviation, i.e.,

$$\left(\frac{\partial K}{\partial[\mathrm{Sb}]}\sigma_{[\mathrm{Sb}]}\right)_{\mathrm{av}} = \frac{\sum_{k=1}^{n} \frac{\partial K}{\partial[\mathrm{Sb}]_k}\sigma_{[\mathrm{Sb}]_k}}{n}, \tag{14}$$

where n is the number of solutions.

3.2. Antimonous acid protonation

From previous studies at 25 °C (Table 1), it is known that a protonated form of antimonous acid, $H_4SbO_3^+$, occurs in acidic aqueous solutions. In order to further study the formation of this species, the spectra of Sb(III)-containing solutions were measured at low pH and at temperatures from 22 to 75 °C using the spectrophotometric titration method. Fig. 3 shows spectra of Sb(III)-containing solutions within the acidic range (pH 0.86–2.27) at 22 °C. Compositions of solutions used to measure spectra at temperatures 22, 50, and 75 °C are given in Appendix Tables A.1, A.2, and A.3. Spectra at high temperatures (i.e., 100, 150, 200, 250, and 300 °C) were collected using a titanium/palladium alloy optical cell as described previously. Fig. 4 shows spectra of Sb-containing solutions within the acidic range at 300 °C and saturated water vapour pressure and Appendix Table A.4 gives the compositions of the acidic antimony-containing solutions for which spectra were measured from 100 to 300 °C. Rank analysis of the absorbance matrix at each temperature demonstrated that three absorbing species were present at all measured temperatures. However, at 250 and 300 °C, the contribution to the total absorbance from the third species was very weak. In order to understand which species were contributing to the overall absorbance envelope, spectra of aqueous solutions containing only perchloric acid with concentrations between 0.0110 and 0.2595 mol/dm^3 (see Appendix Table A.5) were measured from 25 to 300 °C. For the study of the protonation of antimonous acid, aqueous antimony solutions were prepared with perchloric acid concentrations up to 0.2218 mol/dm^3.The molar absorptivities, ε, of ClO_4^- are shown in Fig. 5 and are typical of a charge-transfer-to-solvent (ctts) type of transition. The low energy absorption edge undergoes the expected red shift with increasing temperature (Fig. 5). The ClO_4^- ion absorbs in the wavelength interval 190–240 nm. Consequently, one of the absorbing species present in the solutions is the perchlorate ion, ClO_4^-. However, ClO_4^- ion absorbs weakly, in comparison with the ctts spectra of OH^- and Cl^- ions. Nevertheless, at ClO_4^- concentrations of 0.1–0.2 mol/dm^3, there is a significant contribution from perchlorate ion absorbance to the total measured absorbance. Therefore, this contribution was subtracted from the spectra of all solutions containing perchloric acid at all temperatures.

The chemical model for acidic antimony-containing solutions is given by reaction (1). At 22 °C, the first 10 spectra from pH = 0.85 to 1.00 were identical, i.e., the con-

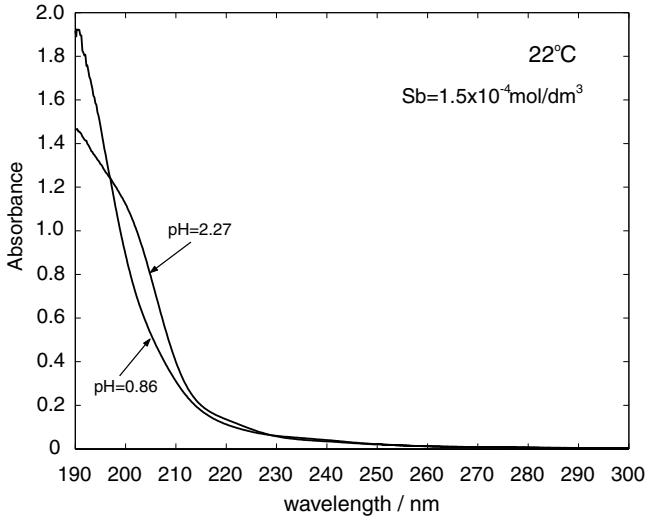

Fig. 3. The spectra at low pH Sb(III)-containing solutions ($Sb = 1.5 \times 10^{-4}$–1.1×10^{-4} mol/dm^3) corrected for water solvent and quartz glass cuvette absorbance at 22 °C; only 2 of 40 measured spectra are shown.

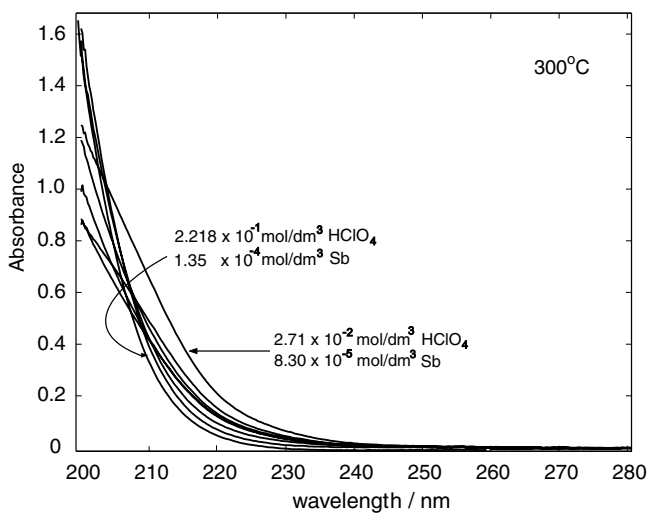

Fig. 4. The spectra at low pH Sb(III)-containing solutions (with $Sb = 1.35 \times 10^{-4}$ mol/dm^3 in the first solution and $Sb = 8.30 \times 10^{-5}$ mol/dm^3 in the last solution) corrected for water solvent and quartz glass windows absorbance at 300 °C and saturated water vapour pressure.

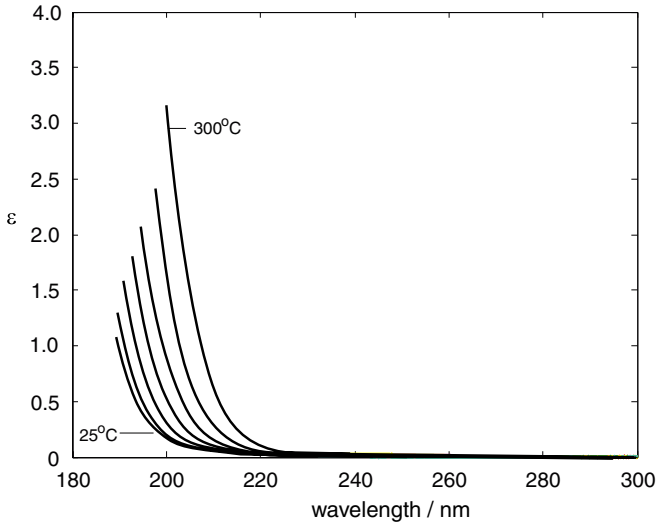

Fig. 5. Molar absorptivities, ε, of ClO_4^- from 25 to 300 °C at the saturated vapour pressure.

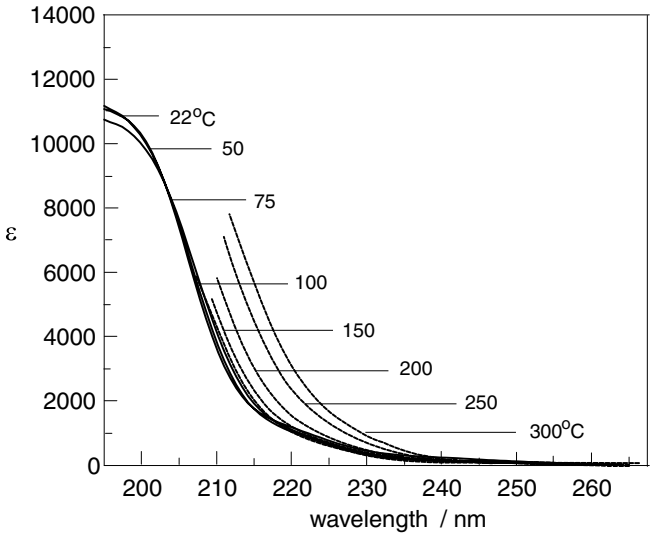

Fig. 7. Molar absorptivity, ε, of $H_3SbO_3^0$ from 22 to 300 °C at the saturated vapour pressure.

centration of the Sb(III)-containing species is independent of pH in this range. Thus, the second of the three absorbing species can be ascribed to the protonated antimonous acid, $H_4SbO_3^+$. Fig. 6 shows the calculated molar absorptivity of the protonated antimonous acid species. It absorbs intensely at low temperatures. With increasing temperature, perchlorate ion molar absorptivity increases at a given wavelength, although the molar absorptivity for the band maximum for the ClO_4^- ion will decrease with increasing temperature. The molar absorptivity of the protonated antimonous acid species, $H_4SbO_3^+$ decreases with increasing temperature. This makes calculation of molar absorptivities at temperatures between 150 and 300 °C less accurate and evaluation of protonation constant difficult. The third absorbing species is neutral antimonous acid. The molar absorptivities determined in this study are shown in Fig. 7. The spectra broaden as temperature

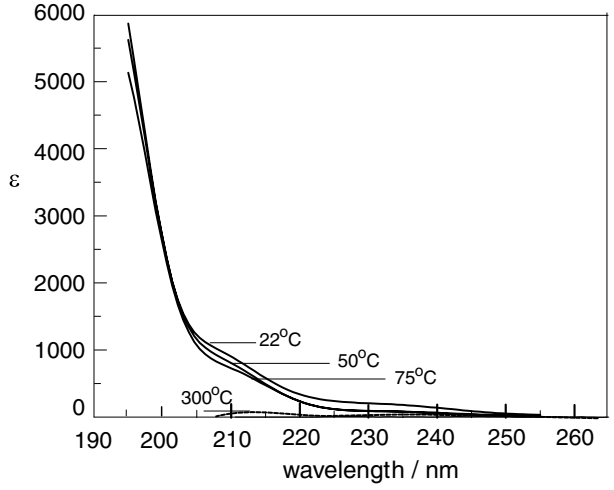

Fig. 6. Molar absorptivities, ε, of $H_4SbO_3^+$ from 22 to 300 °C at the saturated vapour pressure.

increases up to 300 °C. At 22, 50, and 75 °C, the maximum absorption and band position is well defined at about 190 nm. With increasing temperature, the spectra are overlapped by the red-shifted ClO_4^- contribution and the water continuum absorption, which obscure the band maximum for H_3SbO_3 by increasing absorbances to values greater than 2.

The values of the equilibrium constants obtained by the non-linear, non-negative least squares refinement are summarised in Table 2. These values given as a function of temperature were fitted to the equation

$$\log_{10} K_a = a + bT + cT^2 + d/T + e \ln T, \quad (15)$$

where T is in Kelvin. A three-term expression, where $a = 54.5166$, $b = 0.0272$, $e = -10.7494$, was found to best fit the data and was subsequently differentiated to provide values of the standard enthalpy, ΔH°, from

$$\left(\frac{\partial \ln K_a}{\partial T}\right)_p = \frac{\Delta H^\circ}{RT^2}, \quad (16)$$

where R is a gas constant and the entropy change, ΔS°, is obtained in the conventional way from

Table 2
The protonation constant (molal), K_a, of antimonous acid form 22 to 300 °C at saturated vapour pressures, where the uncertainly is 2σ; the values reported here are related to the hypothetical 1 m standard state

t (°C)	$\log K_a$
22	1.385 ± 0.012
50	1.236 ± 0.008
75	1.078 ± 0.009
100	0.94 ± 0.08
150	1.04 ± 0.15
200	1.1 ± 0.3
250	1.5 ± 0.3
300	1.8 ± 0.3

$$\Delta G^\circ = \Delta H^\circ - T\Delta S^\circ. \quad (17)$$

The resulting values of ΔH° and ΔS° for antimonous acid protonation are given in Table 3. In Fig. 8, it can be seen that the equilibrium protonation constant initially decreases with increasing temperature up to 100 °C but then increases until it reaches a value of $\log K_a = 1.8$ at 300 °C. Uncertainties in the determination of the protonation constant at 22, 50, and 75 °C temperatures are remarkably low (see Table 2) because a large number of experimental solutions (up to 60) were studied that allowed a statistically rigorous definition of the spectra for all three species, ClO_4^-, $H_4SbO_3^+$, and $H_3SbO_3^0$. For constants obtained from 100 to 300 °C, uncertainties increase, partly because of the smaller number of solutions studied. With increasing temperature, additional uncertainties can be explained by a combination of changes of molar absorptivities of all three species and possible decomposition of perchloric acid at the highest temperatures, despite having collected the spectra in a flow-through mode. The molar absorptivity of ClO_4^- (Fig. 5) is red-shifted with increasing temperature and strongly overlaps with the absorbance of $H_4SbO_3^+$ (Fig. 6), which also decreases with increasing temperature.

Table 3
Thermodynamic data calculated from our experimental data (see Eqs. (16) and (17)) for antimonous acid protonation (reaction (1)) at the saturated vapour pressure

t (°C)	ΔG° (kJ mol^{-1})	ΔH° (kJ mol^{-1})	ΔS° (J mol^{-1} K^{-1})
22	−7.82	−15.37	−25.6
50	−7.64	−12.12	−13.9
75	−7.17	−8.53	−3.9
100	−6.72	−4.28	6.5
150	−8.40	6.16	34.4
200	−10.28	19.20	62.3
250	−15.02	34.84	95.3
300	−19.74	53.08	127.1

Unfortunately, there are no available thermodynamic data on perchloric acid association. At temperatures below 100 °C, estimates of perchloric acid ionisation are controversial (Haase et al., 1965; Quist et al., 1965). However, association of perchloric acid at high temperatures has already been observed by Ratcliffe and Irish (1984) who studied the Raman spectra of perchloric acid and found traces of molecular $HClO_4$ in concentrated acid solutions. Henderson et al. (1971) studied the kinetics of thermal decomposition of 1.1–6.6 m perchloric acid at 295–322 °C, with the suggested products of decomposition being O_2, Cl_2, and HCl. Since there are no reliable thermodynamic data on perchloric acid association, correction for association was not included in the calculations and the assumption was made that all perchloric acid is ionised. The rank of the absorbance matrix is three, indicating that no other absorbing decomposition products such as Cl_2(aq) or ClO^- are present.

At ambient temperature, our value of $\log K_a = 1.385$ is in good agreement with the spectrophotometrically derived value of $\log K_a = 1.42$ reported by Mishra and Gupta (1968) at $I = 0$. The values of Vasil'ev and Shorokhova (1972) and Popova et al. (1975) (see Table 1) are also in reasonable agreement although the earlier reported value of $\log K_a = 1.17$ by Gayer and Garrett (1952) is apparently a little low.

Equilibrium constants at elevated temperatures for the protonation of antimonous acid reaction estimated by Popova et al. (1975) from solubility measurements are plotted in Fig. 8. The agreement with their values is reasonable up to 100 °C, however, their values diverge from our experimentally determined values with increasing temperature. We are unable to account for the discrepancy.

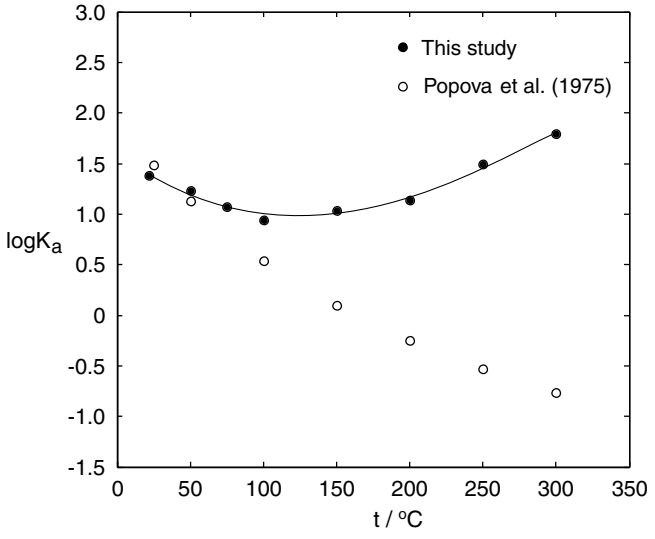

Fig. 8. Variation $\log K_a$ (Eqs. (1) and (5)), for the formation of $H_4SbO_3^+$ at the equilibrium saturated vapour pressure.

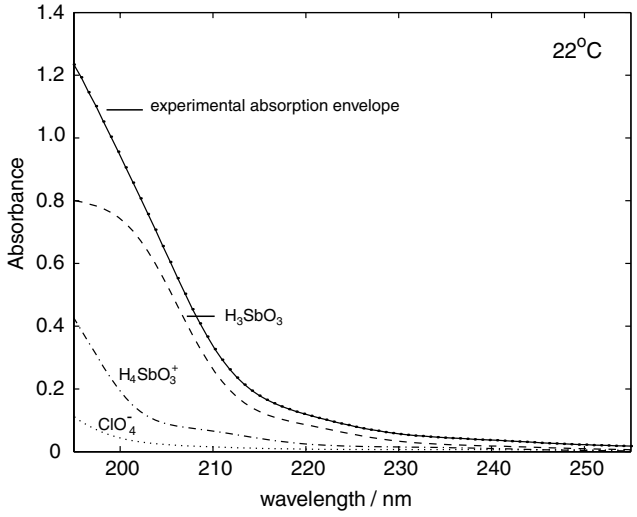

Fig. 9. Deconvoluted spectrum for a solution having pH 1.38 and Sb = 1.20×10^{-4} mol/dm^3 at 22 °C.

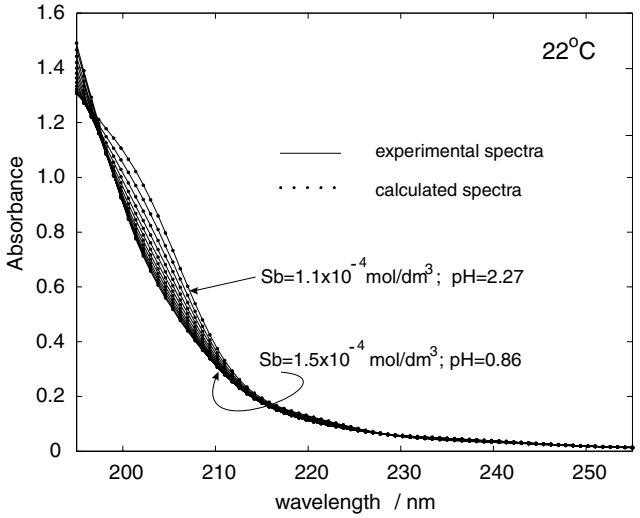

Fig. 10. Experimental (solid lines) and calculated (dots) antimonous acid spectra for a series of solutions within the pH interval from 0.86 to 2.27 and $Sb = 1.5 \times 10^{-4} - 1.1 \times 10^{-4}$ mol/dm^3 at 22 °C.

Fig. 9 shows an example of a deconvoluted spectrum of antimonous acid solution at 22 °C with a total concentration of $Sb = 1.20 \times 10^{-4}$ mol/dm^3 and pH = 1.38. Fig. 10 shows experimental and calculated antimonous acid spectra at room temperature for a series of solutions and illustrates the excellent agreement between the calculated and experimental spectra. This suggests that the chosen chemical model and mathematical description are credible.

3.3. Antimonous acid ionisation

Spectra were collected at temperatures 25, 50, 100, 150, 200, 250, and 300 °C in alkaline solutions. Figs. 11 and 12 show measured spectra of a series of alkaline Sb-containing solutions at 25 and 300 °C at the saturated water vapour pressure. The compositions of the solutions are given in Appendices A.6 and A.7. In all cases, the absorbance increases with increasing sodium hydroxide concentration.

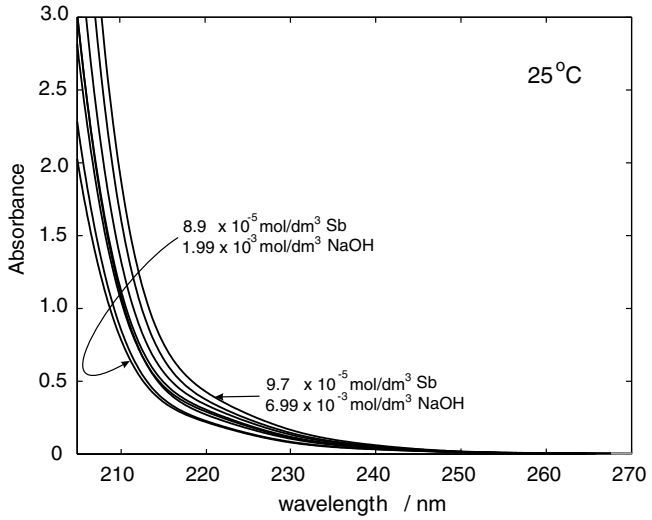

Fig. 11. Antimonous acid spectra in alkaline aqueous solutions at 25 °C.

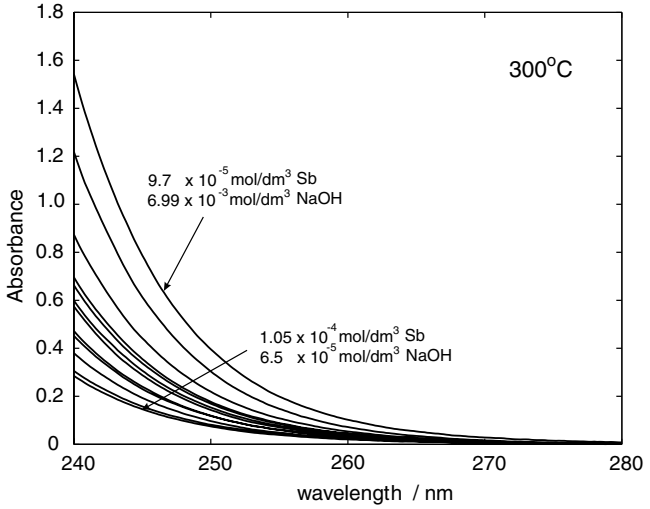

Fig. 12. Antimonous acid spectra in alkaline aqueous solutions at 300 °C at the saturated vapour pressure.

Rank analysis of the absorbance matrix at temperatures from 25 to 300 °C was carried out for all spectra. The rank of the matrix is two at all temperatures from 25 to 300 °C as illustrated for 25 and 300 °C in Fig. 13. For 25 °C, the spectra of eight solutions (Appendix Table A.6) were used to determine the rank. At 300 °C, the spectra of 21 solutions (Appendix Table A.7) were employed in the rank determination. Now we are left to assign the two absorbing species. The solutions contained high concentrations of sodium hydroxide. The hydroxide ion absorbs strongly in the uv in the region from 190 to 220 nm at 25 °C and from 190 to 250 nm at 300 °C as shown previously (Zakaznova-Herzog et al., 2006). That means that it does not absorb in the wavelength range from 220 to 240 nm from 25 to 250 °C, but it absorbs at 240–250 nm at 300 °C, where spectra of Sb-containing solutions were measured, and where results of the rank analysis indicated two absorbing species to be present. We have shown (Fig. 7) that $H_3SbO_3^0$ absorbs in the wavelength interval, 190–240 nm at 250 °C, broadening to 190–250 nm with increasing temperature to 300 °C. Thus, one of the absorbing species in the alkaline antimony-containing solutions from 25 to 250 °C can be assigned to $H_3SbO_3^0$. At 300 °C, one of the absorbing species can be assigned to the hydroxide ion, since $H_3SbO_3^0$ has almost no contribution to the total absorbance at this temperature. This conclusion is based not only on analysis of absorbance interval, but is also supported by the chemical/mathematical model used in the calculation of the deprotonation constant. Thus, the presence of $H_3SbO_3^0$ as an absorbing species at 300 °C is not consistent with the trends observed at other temperatures.

The second absorbing species at all measured temperatures is assigned to the deprotonated antimonous acid ion, $H_2SbO_3^-$. The formation of the polynuclear species is considered unlikely because the concentration of antimony in the solutions was low and always less than 0.00026 mol/dm^3. The strong red shift of the low energy absorption edge of the deprotonated antimonous acid spe-

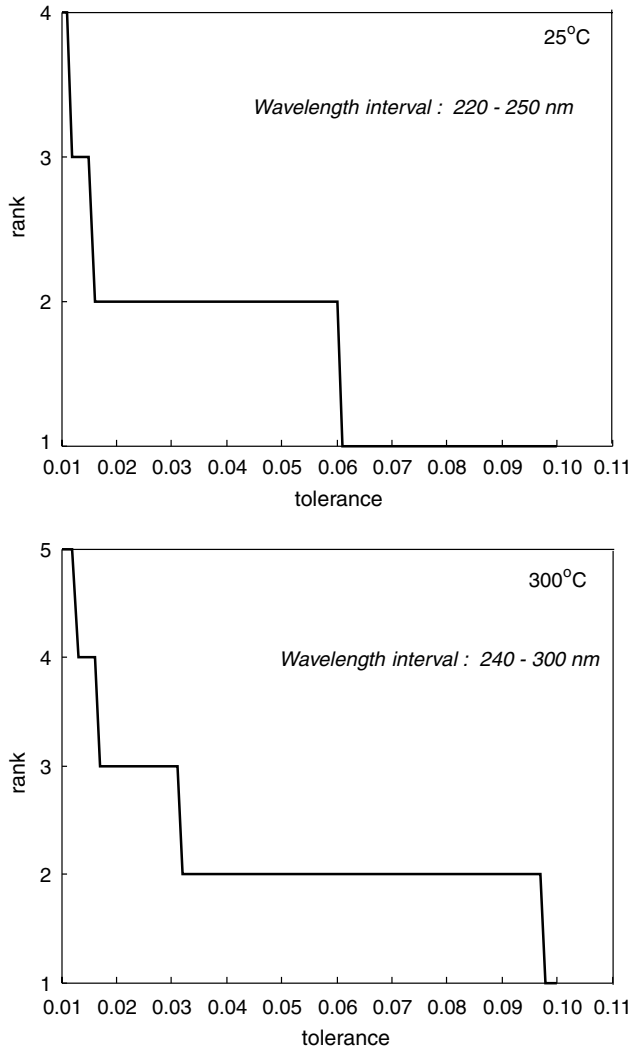

Fig. 13. Determination of the rank of the absorbance matrix for Sb(III)-containing alkaline solutions (Appendices A.6 and A.7) at 25 and 300 °C.

cies with increasing temperature is characteristic of a ctts type of electron transition. Therefore, the deprotonation reaction (reaction (2)) describes the system in this alkaline pH range. The molar absorptivities for the deprotonated antimonous acid species, $H_2SbO_3^-$, from 25 to 300 °C at the saturated vapour pressure are shown in Fig. 14.

The values of the equilibrium constants for the reaction (2) were obtained by the nonlinear non-negative least squares refinement and are summarised in Table 4. Our value ($pK_1 = 11.82$) at 25 °C and $I = 0$ is in good agreement with previously reported values of 11.78 and 11.92 by Gayer and Garrett (1952) and Popova et al. (1975), respectively. With increasing temperature, the deprotonation constant of the antimonous acid (Fig. 15) decreases in a manner similar to that observed for arsenous acid and other weak acids.

The available literature values of equilibrium constants by Popova et al. (1975) are shown in Fig. 15 by the empty circles. These values are based on the recalculation of their solubility data up to 200 °C and are in a reasonable agreement with our data.

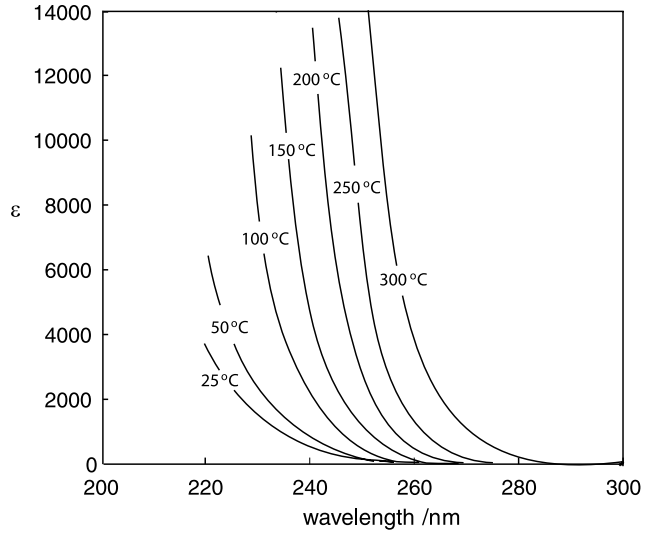

Fig. 14. Molar absorptivities, ε, for $H_2SbO_3^-$ from 25 to 300 °C at the saturated vapour pressure.

Table 4
Ionisation constants, K_1, of antimonous acid (reaction (2)) from 25 to 300 °C at saturated vapour pressures; the uncertainty is 2σ; the values reported here are related to the hypothetical 1 m standard state

t (°C)	pK_1
25	11.82 ± 0.02
50	11.52 ± 0.04
100	11.05 ± 0.02
150	10.56 ± 0.03
200	10.19 ± 0.02
250	9.99 ± 0.02
300	9.88 ± 0.02

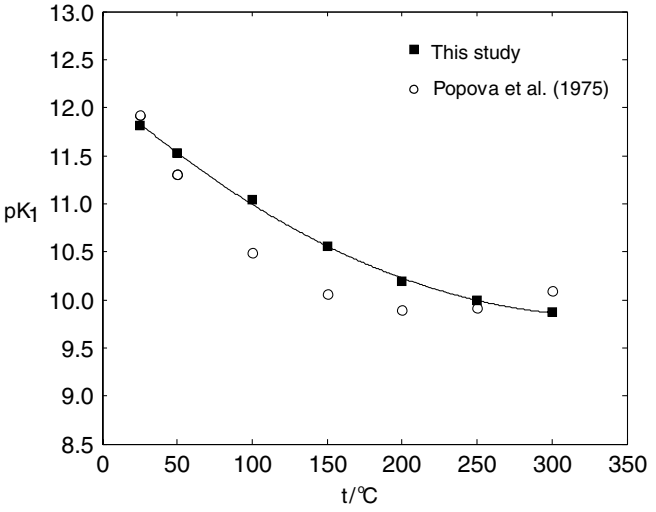

Fig. 15. Temperature dependence of the ionisation constant, K_1, for antimonous acid at the saturated vapour pressure.

In addition, the values of the ionisation constants as a function of temperature were best fitted by the three term version of Eq. (15), where $a = -17.4166$, $b = 0.0247$, and $c = -2.0158 \times 10^{-5}$. The equation was subsequently differ-

entiated to provide values of the standard enthalpy and entropy change of arsenous acid ionisation (Table 5). An example of a deconvoluted spectrum of antimonous acid solution at 25 °C with a total concentration of $Sb = 1.40 \times 10^{-4}$ mol/dm^3 and pH = 11.68 is given in Fig. 16.

Table 5
Thermodynamic data calculated from our experimental data (see Eqs. (16) and (17)) for antimonous acid ionisation (reaction (2)) at the saturated vapour pressure

t (°C)	ΔG° (kJ mol^{-1})	ΔH° (kJ mol^{-1})	ΔS° (J mol^{-1} K^{-1})
25	67.43	17.2	−169
50	71.23	20.1	−158
100	78.90	26.5	−141
150	85.50	33.7	−122
200	92.26	41.7	−107
250	100.0	50.4	−94.8
300	108.4	59.8	−84.7

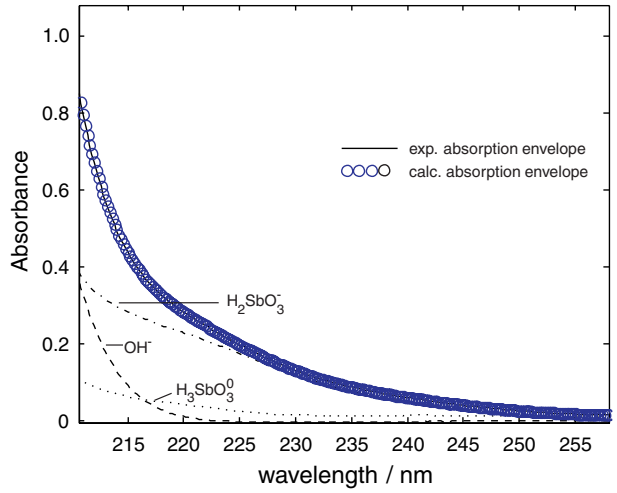

Fig. 16. Deconvoluted spectrum for a solution having $Sb = 1.40 \times 10^{-4}$ mol/dm^3 and pH 11.68 at 25 °C. The solid line refers to the experimental absorption spectrum and the circles to the calculated spectrum.

4. Conclusions

The protonation and deprotonation of antimonous acid from ambient temperature to 300 °C have been studied spectrophotometrically. Log K_a for protonation of antimonous acid varies from 1.38 to 0.94 over a temperature interval from 22 to 100 °C and then increases to 1.8 at 300 °C. The deprotonation constant for antimonous acid decreases dramatically with temperature in a way similar to that observed for arsenous acid by Zakaznova-Herzog et al. (2006). pK_1 constant varied from 11.82 to 9.88 from 25 to 300 °C. Fig. 17 shows the distribution of antimonous acid species in aqueous solutions at 25 and 300 °C as a function of pH.

We note that the dominant antimony (III) species in low sulphur, rock buffered hydrothermal fluids will be H_3SbO_3. However, phase separation and/or boiling leads to an increase in pH and hence the role of $H_2SbO_3^-$ in more alkaline geothermal fluids at elevated temperatures must also be considered. In high sulphidation epithermal ore deposits and other hydrothermal environments exhibiting advanced argillic alteration, low pH fluids are involved at various stages in the evolution of such systems. The $H_4SbO_3^+$ species may play a role in Sb(III) transport and in the deposition of antimony-containing phases (e.g., Sb-containing enargite and luzonite–famatinite solid solutions) in such ore depositing systems.

Acknowledgments

This project was supported by ETH research funding awarded to T.M. Seward. We thank two anonymous reviewers as well as H.L. Barnes and A.V. Zotov for their constructive reviews.

Associate editor: Liane G. Benning

Appendix A

See Tables A.1–A.7.

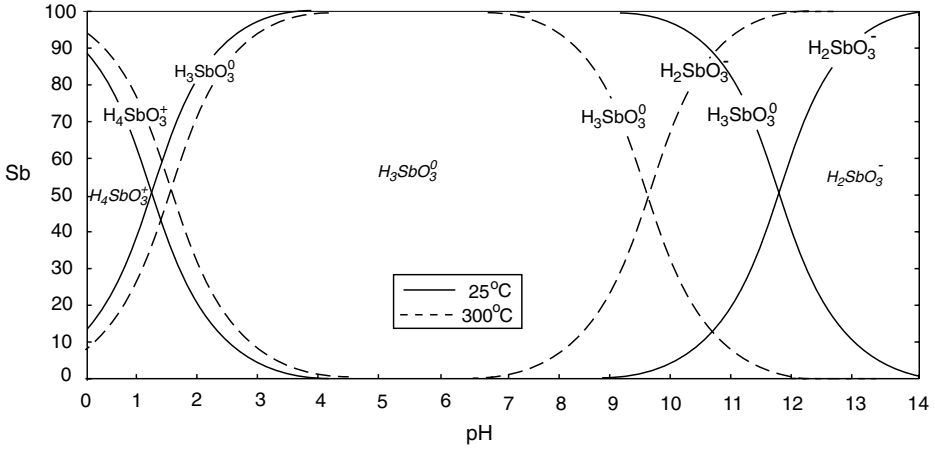

Fig. 17. The distribution of antimonous acid species as a function of pH at 25 and 300 °C at the saturated vapour pressure.

Table A.1
Compositions of 60 experimental solutions used for antimonous acid protonation determination at 22 °C

Solution	∑Sb	ClO_4^-	NaOH	pH
1	0.00015	0.13927	0.00000	0.86
2	0.00015	0.13860	0.00223	0.87
3	0.00015	0.13794	0.00445	0.87
4	0.00015	0.13729	0.00664	0.88
5	0.00014	0.13664	0.00881	0.89
6	0.00014	0.13600	0.01096	0.90
7	0.00014	0.13536	0.01309	0.91
8	0.00014	0.13473	0.01520	0.92
9	0.00014	0.13411	0.01729	0.39
10	0.00014	0.13349	0.01936	0.94
11	0.00014	0.13288	0.02141	0.95
12	0.00014	0.13227	0.02345	0.96
13	0.00014	0.13167	0.02546	0.97
14	0.00014	0.13107	0.02746	0.98
15	0.00014	0.13048	0.02944	1.00
16	0.00014	0.12990	0.03140	1.01
17	0.00014	0.12932	0.03334	1.02
18	0.00014	0.12874	0.03527	1.03
19	0.00014	0.12817	0.03718	1.04
20	0.00014	0.12761	0.03907	1.05
21	0.00013	0.12705	0.04094	1.07
22	0.00013	0.12649	0.04280	1.08
23	0.00013	0.12594	0.04465	1.09
24	0.00013	0.12540	0.04647	1.10
25	0.00013	0.12486	0.04829	1.12
26	0.00013	0.12432	0.05008	1.13
27	0.00013	0.12379	0.05186	1.14
28	0.00013	0.12326	0.05363	1.16
29	0.00013	0.12274	0.05538	1.47
30	0.00013	0.12222	0.05711	1.19
31	0.00012	0.11714	0.05884	1.20
32	0.00012	0.11665	0.06054	1.22
33	0.00012	0.11616	0.06223	1.23
34	0.00012	0.11567	0.06391	1.25
35	0.00012	0.11519	0.06558	1.27
36	0.00012	0.11471	0.06723	1.28
37	0.00012	0.11424	0.06887	1.30
38	0.00012	0.11377	0.07049	1.32
39	0.00012	0.93390	0.07210	1.34
40	0.00012	0.11284	0.07370	1.36
41	0.00012	0.11238	0.07528	1.38
42	0.00012	0.11192	0.07685	1.40
43	0.00012	0.11147	0.07841	1.43
44	0.00012	0.11102	0.07996	1.45
45	0.00011	0.11058	0.08149	1.48
46	0.00011	0.11014	0.08302	1.50
47	0.00011	1.02470	0.08453	1.53
48	0.00011	0.10926	0.08603	1.56
49	0.00011	0.10883	0.08751	1.59
50	0.00011	0.10841	0.08899	1.63
51	0.00011	0.10798	0.09045	1.66
52	0.00011	0.10756	0.09191	1.70
53	0.00011	0.10714	0.09335	1.74
54	0.00011	0.10673	0.09478	1.79
55	0.00011	0.10632	0.09620	1.84
56	0.00011	0.10591	0.09761	1.90
57	0.00011	0.00551	0.09900	1.97
58	0.00011	0.10511	0.10039	2.05
59	0.00011	0.10471	0.10177	2.15
60	0.00011	0.10431	0.10313	2.27

pH is calculated from mass and charge balance equations; concentrations are in mol/dm^3.

Table A.2
Compositions of 62 experimental solutions used for antimonous acid protonation determination at 50 °C

Solution	∑Sb	ClO_4^-	NaOH
1	0.0001605	0.1685	—
2	0.0001598	0.1677	0.00209
3	0.0001591	0.1670	0.00418
4	0.0001584	0.1663	0.00624
5	0.0001577	0.1655	0.00828
6	0.0001570	0.1648	0.01031
7	0.0001563	0.1641	0.01231
8	0.0001556	0.1633	0.01430
9	0.0001549	0.1626	0.01628
10	0.0001543	0.1619	0.01823
11	0.0001536	0.1612	0.02017
12	0.0001529	0.1605	0.02209
13	0.0001523	0.1598	0.02400
14	0.0001516	0.1592	0.02588
15	0.0001510	0.1585	0.02776
16	0.0001503	0.1578	0.02961
17	0.0001497	0.1571	0.03145
18	0.0001491	0.1565	0.03328
19	0.0001485	0.1558	0.03509
20	0.0001478	0.1552	0.03689
21	0.0001472	0.1545	0.03867
22	0.0001466	0.1539	0.04043
23	0.0001460	0.1533	0.04218
24	0.0001454	0.1526	0.04392
25	0.0001448	0.1520	0.04564
26	0.0001442	0.1514	0.04735
27	0.0001437	0.1508	0.04905
28	0.0001431	0.1502	0.05073
29	0.0001425	0.1496	0.05240
30	0.0001419	0.1490	0.05405
31	0.0001414	0.1484	0.05569
32	0.0001408	0.1478	0.05732
33	0.0001403	0.1472	0.05893
34	0.0001397	0.1466	0.06054
35	0.0001392	0.1461	0.00013
36	0.0001386	0.1455	0.06371
37	0.0001381	0.1449	0.06527
38	0.0001375	0.1444	0.06682
39	0.0001370	0.1438	0.06837
49	0.0001319	0.1433	0.06990
41	0.0001360	0.1427	0.07141
42	0.0001354	0.0422	0.07292
43	0.0001349	0.1416	0.07441
44	0.0001344	0.1411	0.07590
45	0.0001339	0.1406	0.07737
46	0.0001334	0.1400	0.07883
47	0.0001329	0.1395	0.08028
48	0.0001324	0.1390	0.08172
49	0.0001319	0.1385	0.08315
50	0.0001314	0.1380	0.08457
51	0.0001309	0.1374	0.08598
52	0.0001305	0.1369	0.08737
53	0.0001300	0.1364	0.08876
54	0.0001295	0.1359	0.09014
55	0.0001290	0.1355	0.13550
56	0.0001286	0.1350	0.09286
57	0.0001281	0.1345	0.09421
58	0.0001237	0.1298	0.12980
59	0.0001199	0.1259	0.11810
60	0.0001191	0.1250	0.14960
61	0.0001183	0.1242	0.12270
62	0.0001179	0.1238	0.12390

Concentrations are in mol/dm^3.

Table A.3
Compositions of 44 experimental solutions used for antimonous acid protonation determination at 75 °C

Solution	$\sum$Sb	ClO_4^-	NaOH
1	0.000159	0.1677	—
2	0.000159	0.1669	0.00231
3	0.000158	0.1661	0.00459
4	0.000157	0.1653	0.00686
5	0.000157	0.1645	0.00911
6	0.000156	0.1637	0.01133
7	0.000155	0.1629	0.01353
8	0.000154	0.1621	0.01570
9	0.000154	0.1613	0.01786
10	0.000153	0.1606	0.02000
11	0.000152	0.1598	0.02211
12	0.000152	0.1590	0.02421
13	0.000151	0.1583	0.02629
14	0.000150	0.1575	0.02835
15	0.000149	0.1568	0.03038
16	0.000149	0.1561	0.01350
17	0.000148	0.1554	0.03441
18	0.000147	0.1547	0.03639
19	0.000147	0.1540	0.03835
20	0.000146	0.1533	0.15330
21	0.000145	0.1526	0.04223
22	0.000145	0.1519	0.04414
23	0.000144	0.1512	0.04603
24	0.000143	0.1505	0.04791
25	0.000143	0.1498	0.04977
26	0.000142	0.1492	0.05162
27	0.009112	0.1485	0.05344
28	0.000141	0.1479	0.05526
29	0.000140	0.1472	0.05705
30	0.000140	0.1466	0.05883
31	0.000139	0.146	0.06060
32	0.000138	0.1453	0.06235
33	0.000138	0.1447	0.06408
34	0.000137	0.1441	0.06580
35	0.000137	0.1435	0.06751
36	0.000136	0.1429	0.06920
37	0.000136	0.1423	0.07088
38	0.000135	0.1417	0.07254
39	0.000134	0.1411	0.07419
40	0.000134	0.1405	0.07582
41	0.000129	0.1349	0.09145
42	0.000124	0.1297	0.12970
43	0.000119	0.1249	0.12490
44	0.000118	0.1239	0.12180

Concentrations are in mol/dm^3.

Table A.4
Compositions of eight experimental solutions used for antimonous acid protonation determination from 100 to 300 °C

Solution	$\sum$Sb	ClO_4^-
1	0.000135	0.22180
2	0.000083	0.18963
3	0.000094	0.15424
4	0.000092	0.10967
5	0.000087	0.08572
6	0.000076	0.05326
7	0.000103	0.04827
8	0.000083	0.02713

Concentrations are in mol/dm^3.

Table A.5
Compositions of six experimental solutions obtain for calculating molar absorptivities of ClO_4^- ion from 25 to 300 °C

Solution	ClO_4^-
1	0.0110
2	0.0278
3	0.0551
4	0.1158
5	0.1661
6	0.2595

Concentrations are in mol/dm^3.

Table A.6
Compositions of experimental solutions used for antimonous acid deprotonation determination at 25 °C

Solution	$\sum$Sb	NaOH
1	0.000089	0.001994
2	0.000089	0.002528
3	0.000097	0.002570
4	0.000097	0.002804
5	0.000097	0.003088
6	0.000097	0.003972
7	0.000097	0.005572
8	0.000097	0.006992

Concentrations are in mol/dm^3.

Table A.7
Compositions of 21 experimental solutions used for antimonous acid deprotonation determination from 50 to 300 °C

Solution	$\sum$Sb	NaOH
1	0.000105	0.000065
2	0.000262	0.000162
3	0.000105	0.000189
4	0.000096	0.000252
5	0.000138	0.000313
6	0.000094	0.000403
7	0.000144	0.000490
8	0.000113	0.000562
9	0.000069	0.000798
10	0.000107	0.001257
11	0.000120	0.001332
12	0.000089	0.001513
13	0.000089	0.001620
14	0.000089	0.001994
15	0.000089	0.002528
16	0.000089	0.002570
17	0.000097	0.002804
18	0.000097	0.003088
19	0.000097	0.003972
20	0.000097	0.005572
21	0.000097	0.006992

Concentrations are in mol/dm^3.

References

Ahrland, S., Bovin, J., 1974. The complex formation of antimony (III) in perchloric acid and nitric acid solutions. A solubility study. *Acta Chem. Scand. A* **28**, 1089–1100.

Baes, C.F., Mesmer, R.E., 1976. *The Hydrolysis of Cations*. Wiley–Interscience, New York.

Bradley, D.J., Pitzer, K.S., 1979. Thermodynamics of electrolytes. 12. Dielectric properties of water and Debye–Hückel parameters to 350 °C and 1-kbar. *J. Phys. Chem.* **83**, 1599–1603.

Filella, M., Belzile, N., Chen, Y.W., 2002. Antimony in the environment: a review focused on natural waters I. *Occurrence Earth Sci. Rev.* **57**, 125–176.

Gayer, K.H., Garrett, A.B., 1952. The equilibria of antimonious oxide(rhombic) in delute solutions of hydrochloric acid and sodium hydroxide at 25 °C. *J. Am. Chem. Soc.* **74**, 2353–2354.

Gmelin, 1950. *Handbook of Inorganic Chemistry*, vol. 18(A).

Haar, L., Gallagher, J.S., Kell, G.S., 1984. *NBS/NRC Steam tables. Thermodynamic and transport properties and computer programs for vapour and liquid states of water in SI units*. Hemisphere, New York.

Haase, R., Ducker, K.H., Kuppers, H.A., 1965. Aktivitatskoeffizienten und Dissoziationskonstanten wassriger Salpetersaure und Uberchlorsaure. *Ber. Buns. Gesellsch. Physikal. Chem.* **69**, 97.

Helgeson, H.C., Kirkham, D.H., 1974. Theoretical prediction of thermodynamic behavior of aqueous electrolytes at high pressures and temperatures. 2. Debye–Hückel parameters for activity-coefficients and relative partial molal properties. *Am. J. Sci.* **274**, 1199–1261.

Henderson, M.P., Miasek, V.I., Swaddle, T.W., 1971. Kinetics of thermal decomposition of aqueous perchloric acid. *Can. J. Chem.* **49**, 317–324.

Ho, P.C., Bianchi, H., Palmer, D.A., Wood, R.H., 2000. Conductivity of dilute aqueous electrolyte solutions at high temperatures and pressures using a flow cell. *J. Sol. Chem.* **29**, 217–235.

Jander, G., Hartmann, H.J., 1965. Lichtabsorptions-and Diffusionsversuche sowie die Bestimung des Ionenladungsvorzeichens im Sauren Bereich. *Zeit. Anorgan. Allgem. Chem.* **339**, 239–247.

Kielland, J., 1937. Individual activity coefficients of cations in aqueous solutions. *J. Am. Chem. Soc.* **59**, 1675–1678.

Mishra, S.K., Gupta, Y.K., 1968. Spectrophotometric study of the hydrolytic equilibria of Sb(III) in aqueous perchloric acid solution. *Ind. J. Chem.* **6**, 757–758.

Popova, M.Ya., Khodakovsky, I.L., Ozerova, N.A., 1975. Experimental determination of the thermodynamic properties hydroxo- and hydroxofluoride complexes of antimony at temperatures up to 200 °C. *Geokhimiya* **6**, 835–843.

Quist, A.S., Marshall, W.L., Jolley, H.R., 1965. Electrical conductances of aqueous solutions at high temperature and pressure. 2. Conductances and ionization constants of sulfuric acid–water solutions from 0 to 800 °C and at pressures up to 4000 bars. *J. Phys. Chem.* **69**, 2726.

Ratcliffe, C.I., Irish, D.E., 1984. Vibrational spectral studies of solutions at elevated temperatures and pressures. VI. Raman studies of perchloric acid. *Can. J. Chem.* **62**, 1134–1144.

Robinson, R.A., Stokes, R.H., 1968. *Electrolyte solutions*. Butterworths, London.

Vasil'ev, V.P., Shorokhova, V.I., 1972. Determination of the standard thermodynamic characteristics of the antimonyl ion SbO^+ and antimony oxide by a potentiometric method. *Electrokhimiya* **8**, 185–190.

Vasil'ev, V.P., Shorokhova, V.I., 1973. Determination of the thermodynamic characteristics of antimony (III) in alkaline solutions by a solubility method. *Rus. J. Inorg. Chem.* **18**, 161–164.

Weissberg, B.G., Browne, P.R.L., Seward, T.M., 1979. Geochemistry of hydrothermal ore deposits. In: Barnes, H.L. (Ed.), *Ore metals in active geothermal systems*. Wiley, New York, pp. 738–780.

Zakaznova-Herzog, Seward, T.M., Suleimenov, O.M.. Arsenous acid ionisation in aqueous solutions from 25 to 300 °C. *Geochim. Cosmochim. Acta* **70**, 1928–1938.

Zotov, A.V., Shikina, N.D., Akinfiev, N.N., 2003. Thermodynamic properties of the Sb(III) hydroxide complex $Sb(OH)_3(aq)$ at hydrothermal conditions. *Geochim. Cosmochim. Acta* **67**, 1821–1836.